Implementation and Control of an AC/DC/AC Converter for Electric Vehicle Application

H. Schettino, V. Gama, R. Carvalho, J. G. Oliveira, H. Bernhoff

***Abstract*— An all-electric driveline based on a double wound flywheel, connected in series between main energy storage and a wheel motor, is presented. The flywheel works as a power buffer, allowing the battery to deliver optimized power. It also separates electrically the system in two sides, with the battery connected to the low voltage side and the wheel motor connected to the high voltage side.**

This paper presents the implementation and control of the AC/DC/AC converter, used to connect the flywheel high voltage side to the wheel motor. The converter general operation and the adopted control strategy are discussed. The implementation of the AC/DC/AC converter has been described from a practical perspective. Results from experimental tests performed in the full system prototype are presented. The prototype system is running with satisfactory stability during acceleration mode. Good efficiency and unity power factor could be achieved, based on vector control and space vector modulation,

I. Introduction

EXTENSIVE research has been recently done on Electric Vehicles (EVs) [1, 2]. The development of an efficient and robust propulsion system is essential to the feasibility of EVs [3]. But, even though sophisticated engines and advanced electrical power trains exist, the main issue, the long-term energy storage, has not been resolved.

All-electric drivelines based on battery, super-capacitor, flywheel and combinations of these are being widely discussed and tested, attempting to lower the requirement on power density from the batteries [4, 5].

The propulsion system in development at Uppsala University is based upon a double wound flywheel energy storage device [6]. The flywheel under study is physically divided into two voltage levels through the winding stator. The high voltage side of the flywheel is connected to the wheel motor whereas the low voltage side is connected to the battery, as shown in Fig. 1. The system is bidirectional and the power can either flow from the battery to the wheel motor (acceleration mode) or from the wheel-motor to the battery (regenerative braking) [7].

Manuscript received April 15, 2011. This work was supported in part by Ångpanneföreningens Forskningstiftelse and the Swedish Energy Agency (STEM).

H. Schettino, V. Gama and R. Carvalho are with the Electrical Engineering Department, Federal University of Juiz de Fora, CEP 36036-330, Juiz de Fora, Brazil (e-mail: henrique.schettino@engenharia.ufjf.br).

J. G. Oliveira and H. Bernhoff are with the Division for Electricity, Dep. of Eng. Sciences, Uppsala University, Box 534, SE-75121 Uppsala, Sweden (email: janaina.goncalves@angstrom.uu.se).

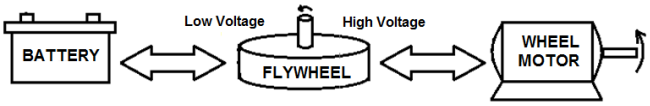

Fig. 1. All-electric driveline schematics: The power can flow in both directions.

In acceleration mode, the flywheel function is basically to absorb the variant power requested by the wheel motor, so that the battery delivers a smoother output power. In braking mode, the wheel motor acts as a generator, and the flywheel is responsible for storing the regenerated energy.

The system needs a considerable number of power electronics converters and electronic controllers in order to regulate and optimize the power flux between the components [8]. A DC/DC converter and a DC/AC converter are used to connect the battery to the flywheel low voltage side. An AC/DC/AC converter is used to connect the flywheel high voltage side to the wheel motor.

This paper presents the implementation and control of the AC/DC/AC converter to link the flywheel high voltage side to the wheel motor. Although it is a bi-directional converter, only the acceleration mode is studied in the present paper. Section II describes the modeling and general operation of the converter. The adopted control strategy is discussed in details in Section III. A prototype system is presented in Section IV and the experimental results are discussed in Section V.

II. The AC/DC/AC Converter

Both the wheel motor and the flywheel machine are three-phase synchronous machines in the present system. The angular speed of synchronous machines is proportional to the applied electric frequency in steady state. The energy stored in the flywheel rotor is related to its angular speed. The wheel motor speed must vary accordingly the vehicle's requirements.

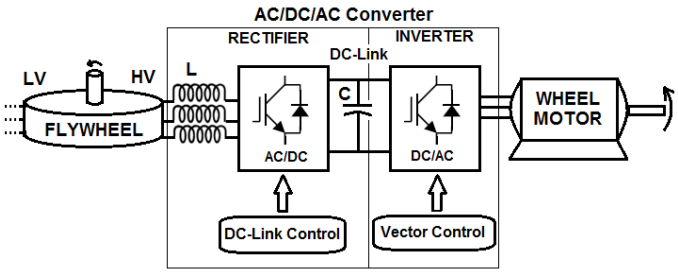

Fig. 2. The AC/DC/AC converter in acceleration mode.

The AC/DC/AC converter is an electrical way to decouple the two frequencies. Two identical three-phase bridges, one capacitor and inductors compose the power circuit. In acceleration mode, the AC/DC/AC converter can be divided into a rectifier and an inverter, as show Fig. 2. This section presents briefly the modeling and functioning of the two modules.

A. *Rectifier*

A forced-commutated three-phase controlled rectifier is required to obtain a desired voltage in the DC-link for different flywheel speeds and different wheel motor loads [9]. A scheme of the forced-commutated rectifier, based on transistors, is shown in Fig. 3.

The AC/DC converter must behave like a voltage boost in order to work as a forced-commutated rectifier. In other words, the DC-Link voltage must be larger than the peak DC voltage generated by the rectifying diodes in passive mode. The inductance L performs the boost voltage operation in combination with the capacitor C and acts at the same time as a low-pass filter for the AC line current. Therefore, the choice of L and C values are extremely important for the proper functioning of the rectifier. Since the flywheel has a very small internal inductance, external inductors need to be placed.

Assuming that the source (Flywheel machine) is a balanced, sinusoidal three phase voltage supply with frequency ω, the input voltages can be written as

$$e_a = -E\sin(\omega t) \tag{1}$$

$$e_b = -E\sin(\omega t - 2\pi/3) \tag{2}$$

$$e_c = -E\sin(\omega t + 2\pi/3)\,. \tag{3}$$

In the rotating *d-q* frame, the input voltage is usually in the quadrature axis [10]. Therefore, the direct component is null.

$$e_d = 0 \tag{4}$$

$$e_q = E \tag{5}$$

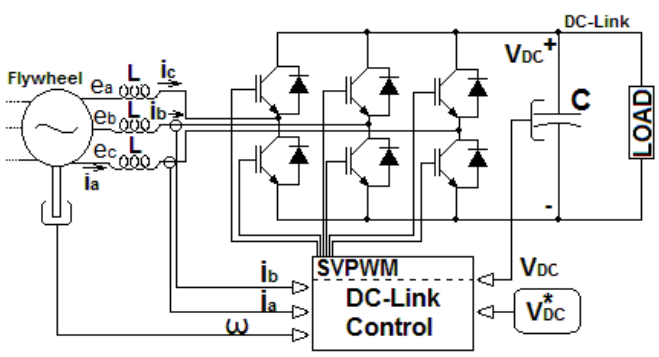

Fig. 3. Forced-commutated three-phase controlled rectifier.

The voltage equation in the rotating *d-q* frame are given by

$$0 = L\frac{di_d}{dt} - \omega L i_q + V_d \tag{6}$$

$$E = L\frac{di_q}{dt} + \omega L i_d + V_q\,. \tag{7}$$

The active power supplied from the source is:

$$P = \frac{3}{2}(e_q i_q + e_d i_d) = \frac{3}{2}E i_q\,. \tag{8}$$

If the i_d current is controlled to zero, the line current is completely represented by i_q component and the active power coming from the source is maximized. Consequently, the input current will be in phase with the input voltage (unity power factor).

$$i_d{}^* = 0. \tag{9}$$

The idea of the proposed control strategy is to control the DC voltage in combination with the input AC currents so that unity power factor is reached. Instantaneous value of the DC voltage, input currents and flywheel speed must be known to achieve closed loop control, as seen in Fig. 3. The control strategy adopted is discussed in detail in Section III.

B. *Inverter*

The inverter scheme is shown in Fig. 4. The AC/DC converter, previously explained, is represented by a DC voltage source in Figure 4.

The inverter is responsible for driving the wheel motor, controlling its angular speed for different load torques. Since the wheel motor is a synchronous permanent magnetic machine (PMSM), the electromagnetic torque expressed in the *d-q* rotating frame is given by [11]:

$$T_e = \frac{3p}{2}[\psi_{PM} i_q + i_q i_d (L_d - L_q)] \tag{10}$$

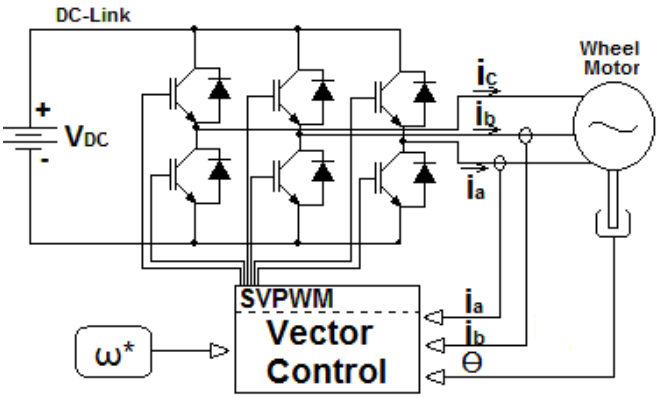

Fig. 4. Inverter.

where p is the number of pole pairs; ψ_{PM} is the flux produced by the permanent magnet; L_d and L_q are respectively the direct and quadrature components of the wheel motor inductance.

Considering a non-salient pole machine (smooth air gap), L_d and L_q are the same, and (9) can be written as

$$T_e = \frac{3p}{2}\psi_{PM} i_q = K i_q . \quad (11)$$

According to Equation (11), only the i_q component can influence the value of the electromagnetic torque produced in the machine. Thus, the maximum torque per ampere occurs when i_q is at its maximum value and, consequently, i_d is equal to zero.

$$i_d{}^* = 0. \quad (12)$$

The implementation of the inverter control requires the feedback signals of the line currents and rotor position instantaneous values, as shown Fig. 4. The details of the control strategy are further explained in Section III.

III. Control Strategy

A. DC-Link Control

A simplified diagram of the DC-link control is shown in Figure 5. Due to the characteristic of closed loop, it is necessary to measure the stator currents and rotor angular position. These measurements are carried out by two current sensors and a hall sensor used to calculate the speed and estimate the rotor position. The instantaneous values of stator currents i_a and i_b are mathematically transformed (Clarke and Park transformations) and then used as the feedback for i_q and i_d control loops.

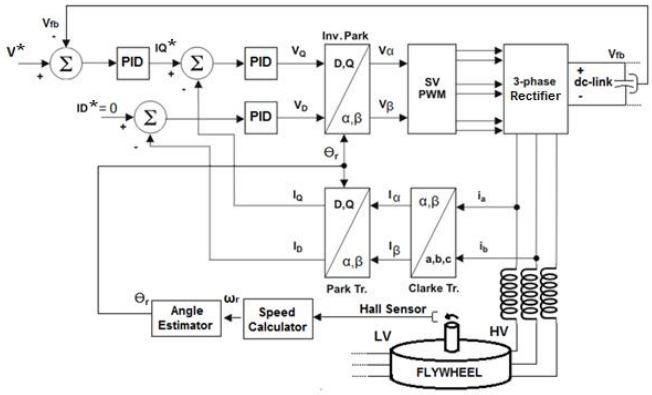

Fig. 5. Block diagram of the DC-Link control.

An outer loop of voltage is connected to a PID regulator. The output of the voltage controller is the reference of the quadrature current i_q. The reference of the direct current i_d is set to zero, in order to obtain unity power factor operation. The output of i_q and i_d PID controllers are transformed into α and β components (Inv Park) and modulated by Space Vector modulation, generating the pulses which are inserted into a three-phase bridge rectifier.

B. Vector Control

The Vector control block diagram is similar to the DC-Link diagram, as shown in Fig.6. Current sensors are necessary to capture the instantaneous values of the line currents. In this case, an encoder was used to measure the rotor angular position. The two inner currents loops are maintained in exactly the same way as for the DC-link control. The main difference is in the outer loop, where a speed loop control is implemented. The output of the speed controller is the reference quadrature current i_q, which regulates the torque needed to reach the reference speed. The reference of the direct current i_d is set to zero, in order to obtain maximum torque per ampere in the machine.

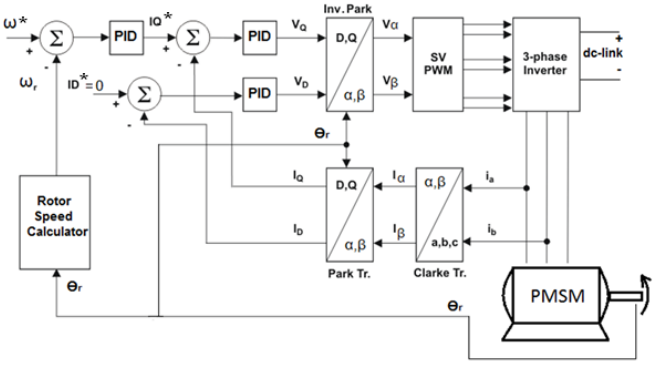

Fig. 6. Block diagram of the Vector control.

IV. Prototype System

A scaled experimental test set-up is being constructed to investigate the properties of the proposed flywheel system [12]. The experiment allows measurements of complete drive cycles to be performed, improving the understanding of the constituting components and optimization of the complete system.

A prototype of the described AC/DC/AC converter which connects the high voltage of the flywheel machine to the wheel motor has been implemented.

A 3.5kW/380V PMSM (manufacturer *Leroy Somer*) is used as wheel motor. The double wound flywheel is a prototype developed at Uppsala University. A DC power supply emulates a battery, connected through a DC/AC converter to the low voltage side of the flywheel (not shown in the diagram).

The high voltage side of the flywheel is connected to 600μH inductors per phase, required for the functionality of the forced-commutated rectifier. A 20mF/350V capacitor is connected in parallel with the DC-Link.

Two three-phase *MOSFET* bridges were built with discrete *DSEI 2130*. A *snubber* circuit was implemented in order to eliminate the rings presented in the *MOSFET* output.

The control of the AC/DC/AC converter has been performed using two MCUs (Microcontrollers) Piccolo

TMDSCNCD28035 (manufactured by Texas Instruments) plugged in the TMDSDOCK28035 Experimenter's Kit.

The current setup has two MCU and two computers, which perform real-time debug, through a USB connection to each computer, as shown in Fig. 7. Although this setup is better for debugging in testing phase, it can be upgraded to one MCU system, without any need for an external computer.

Two mainboards, one for each module of the converter, contain the driver and sensor circuits. The driver used is a IR2130, from *International Rectifier*. With the purpose of avoiding damage in the low power system, the driver was electrically isolated from the MCU by digital optocouplers (A4800). The system requires a large number of sensors: four current sensors (HAL50-S), one encoder (ERN423), one voltage sensor (resistive divider) and three hall sensors (A1101). The current sensors are used in both boards to capture the instantaneous values of the line AC currents. The hall sensor (flywheel speed capture) and the voltage sensor (DC-Link voltage capture) are used for the rectifier control strategy. The encoder is used to estimate the wheel motor rotor angle for the inverter board. The black arrows in Fig. 7 indicate the sensor signals flux.

Different voltage sources are used to feed drivers and sensors. DC/DC Traco-power converters are used to obtain these voltages and isolate the different system components.

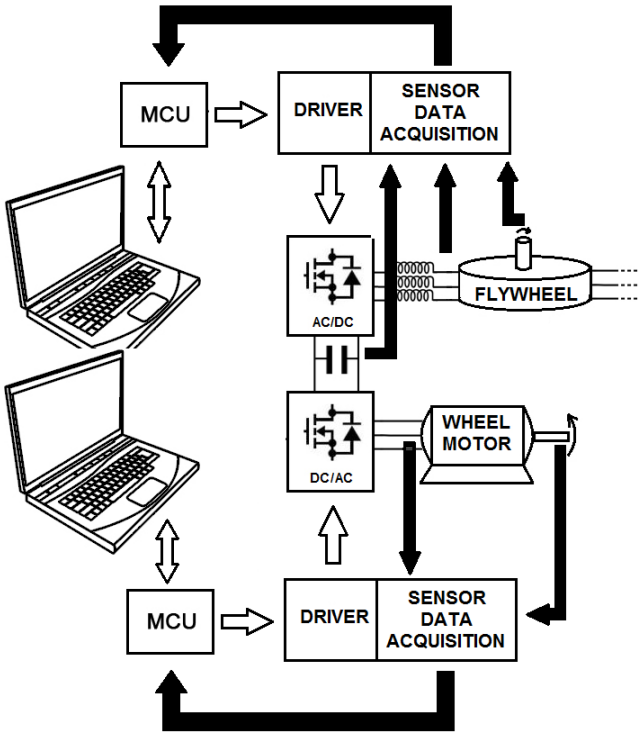

Fig. 7. Prototype System, the black arrows indicate the sensor signals flux.

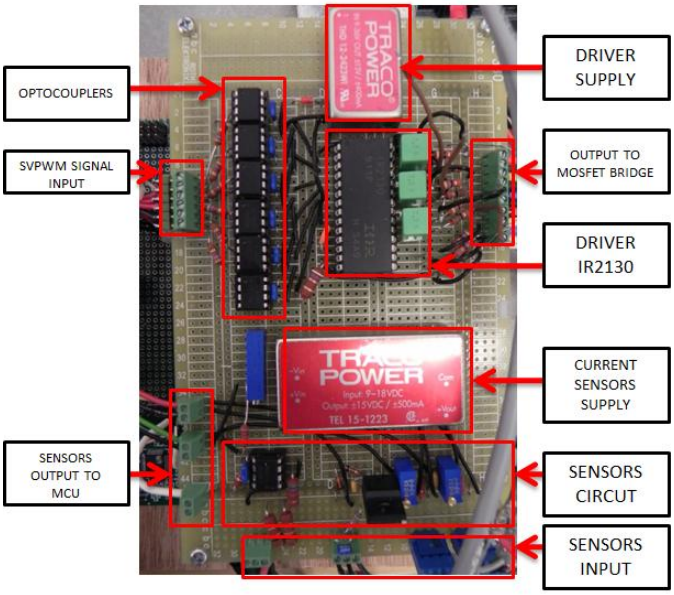

Fig. 8. Rectifier main circuit board.

The rectifier main board with the components indications is shown in Fig. 8. Small changes can be seen in the inverter mainboard due to the different sensors used.

V. Experimental Results

The experimental waveforms for a 20 seconds test performed in the full system prototype are shown in Fig. 9, Fig 10, Fig 11 and Fig 12. A variant torque is applied to the wheel motor up to t = 11 s, as shown in Fig. 9. While the torque is being applied, a stationary error of about 11% compared to the setpoint values occurs in the DC-link voltage control (Fig. 10) and in the motor speed control (Fig. 11).

The flywheel speed decreases from 1950 RPM to 1650 RPM in order to supply the power requested by the wheel motor, as seen in Figure 11. When the torque is changed to a small constant value (t > 11 s), the flywheel speed increases to the initial value (1950 RPM). The DC-link voltage and the speed of the wheel motor coincide with the reference values.

The approximate input and output power curves can be seen in Fig. 12. The mean input power, measured in the terminals of the DC power supply, is 140W and the mean output power, measured from voltage and current supplied to the wheel motor, is 125W. Thus, an efficiency of 89% is achieved.

The line voltage and line current in the flywheel high voltage side (side which is connected to the rectifier) are shown in Fig. 13. The two waves are approximately in phase due to the rectifier control, confirming a unity power factor operation.

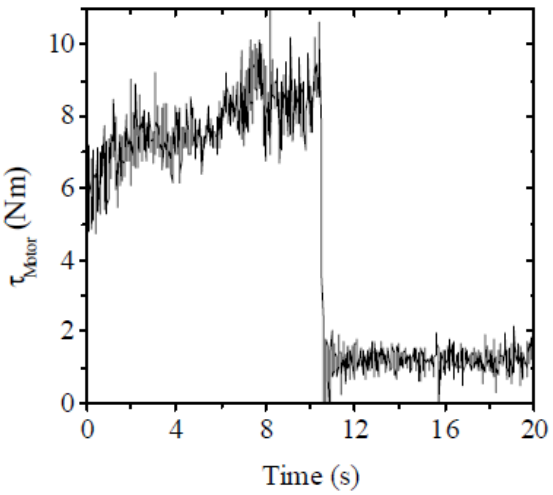

Fig. 9. Applied torque.

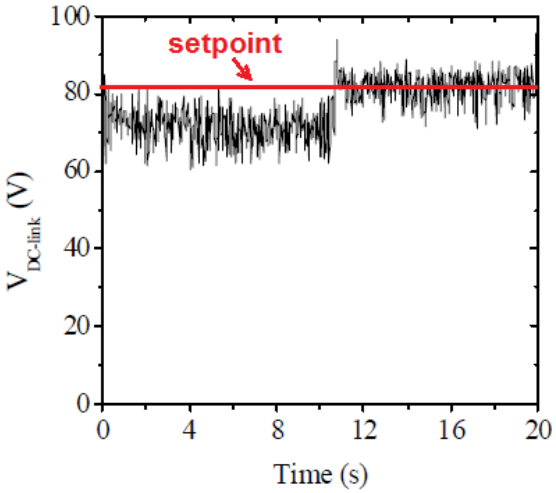

Fig. 10. DC-Link voltage.

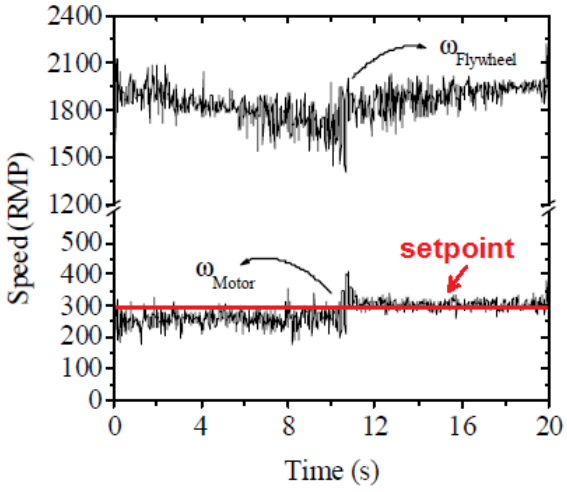

Fig. 11. Flywheel and wheel motor angular speed.

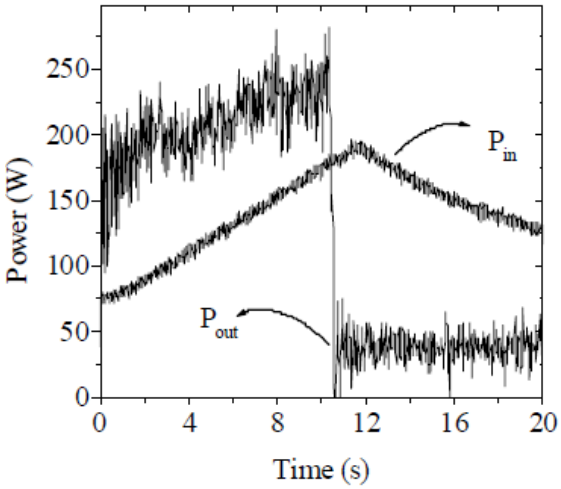

Fig. 12. Input and output power.

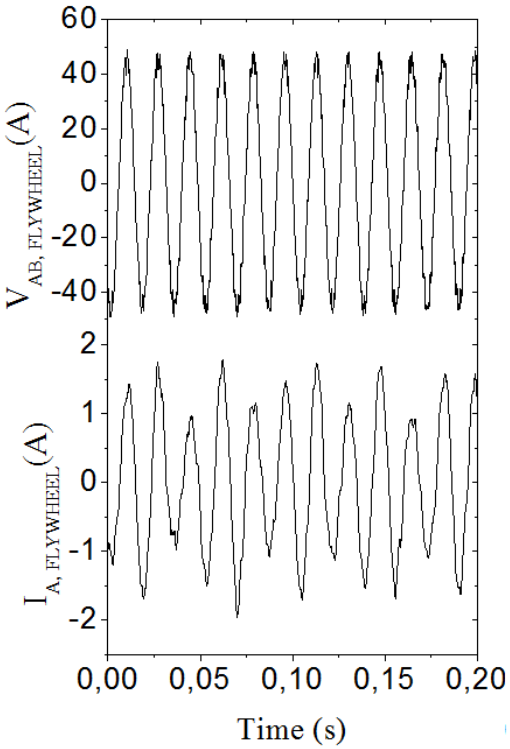

Fig. 13. Line voltage and line current in the flywheel.

VI. Conclusion

An AC/DC/AC converter based on MOSFET modules for double wound flywheel application is presented. The prototype system is running with satisfactory stability in acceleration mode. Some changes in the control system must be implemented in order to achieve regenerative braking. Based on vector control theory and space vector modulation, good efficiency and unity power factor could be achieved.

ACKNOWLEDGMENT

The authors gratefully acknowledge the members of the Electrical Engineering Tutorial Education Program (PET-Elétrica) for the opportunity and encouragement. Thanks also to Juan de Santiago and Francisco José Gomes for the important contributions.

REFERENCES

[1] J. Dixon, “Energy Storage for Electric Vehicles”, IEEE International Conference on Industrial Technology, pp. 20-26, 2010.

[2] P. Fairley, “Speed bumps ahead for electric-vehicle charging”, IEEE Spectrum, vol.: 47, Issue: 1, pp. 13-14, 2010.

[3] A. Emadi, S. S. Williamson and A. Khaligh, “Power electronics intensive solutions for advanced electric, hybrid electric, and fuel cell vehicular power systems”, IEEE Transactions on Power Electronics, vol. 21, no. 3, May 2006.

[4] J. Mierlo, P. Bossche, G. Maggetto, Models of energy sources for EV and HEV: fuel cells, batteries, ultracapacitors, flywheels and enginegenerators, Journal of Power Sources, vol 128, pp 76–89, 2004.

[5] J. Santiago, J. G. Oliveira, J. Lundin, J. Abrahamsson, A. Larsson, H. Bernhoff, "Design parameters calculation of a novel driveline for electric vehicles", World Electric Vehicle Journal Vol. 3 ISSN 2032-6653 - 2009 AVERE.

[6] J. Santiago, A. Larsson, H. Bernhoff (2010) "Dual Voltage Driveline for Vehicle Applications," International Journal of Emerging Electric Power Systems: Vol. 11: Iss. 3, Article 1.

[7] J. G. Oliveira, J. Lundin, J. Santiago, H. Bernhoff, "A Double Wound Flywheel System under Standard Drive Cycles: Simulations and Experiments," *International Journal of Emerging Electric Power Systems*, vol. 11: Iss. 4, Article 6, 2010.

[8] J. G. Oliveira, H. Bernhoff, “Power electronics and control of two-voltage-level flywheel based all-electric driveline”, IEEE International Symposium on Industrial Electronics, 2011.

[9] M. H. Rashid, *Power Electronics Handbook*, Academic Press, 2001.

[10] J. Choi; S. Sul; “Fast Current Controller in 3 -Phase AC/DC Boost Converter Using d-q Axis Cross-Coupling”, 27th Annual IEEE Power Electronics Specialists Conference, vol.1, pp. 177 – 182, 1996.

[11] K. S. Low, M. F. Rahman, K. W. Lim, ‘The dq transformation and feedback linearization of a permanent magnet synchronous motor’, Proceedings of International Conference on Power Electronics and Drive Systems, 1995, 1, pp. 292-296.

[12] J. Abrahamsson, J. Santiago, J. G. Oliveira, J. Lundin, H. Bernhoff, “Prototype of electric driveline with magnetically levitated double wound motor”, Proceedings of the International Conference on Electrical Machines (ICEM), 2010.